内部波ビームの3次元的不安定性

神戸大学 (Kobe University)　　片岡　武 (Kataoka, T.)
Massachusetts Institute of Technology　　Akylas, T. R.

要旨

The stability of isolated and interacting internal gravity wave beams to three-dimensional perturbations is studied, based on the beam–mean-flow interaction equations derived in Kataoka and Akylas (2015). These two-dimensional states are found to be unstable as a result of modulational instability, a purely inviscid mechanism, as well as due to a streaming effect brought about by viscous attenuation along the beam propagation direction.

1. 緒言

Internal gravity wave beams (IGWB) are time-harmonic plane waves with general spatial profile. Such disturbances are manifestations of the anisotropy of internal wave motion in fluids with continuous vertical stratification, and may be regarded as the analogues of cylindrical wavefronts in isotropic media. IGWB are of considerable geophysical interest, as they form the backbone of the internal tide in oceans and can also arise in the atmosphere due to thunderstorms.

Most prior studies of IGWB have focused on two-dimensional (2D) disturbances in an inviscid Boussinesq fluid with constant buoyancy frequency. Under these flow conditions, isolated uniform IGWB happen to be exact nonlinear states irrespective of the beam profile (Tabaei and Akylas 2003), and significant nonlinear interactions may occur in connection with reflections at boundaries and possibly due to collisions of beams (Tabaei et al. 2005). However, the three-dimensional (3D) propagation of IGWB differs fundamentally from its 2D counterpart: 3D variations enable resonant transfer of energy, through the action of Reynolds stresses, to the flow mean vertical vorticity, resulting in strong nonlinear coupling between an IGWB and its induced mean flow. This 3D interaction mechanism is governed asymptotically by two coupled nonlinear amplitude equations (Kataoka and Akylas 2015, hereinafter referred to as KA), which account for the observed strong horizontal mean flow accompanying a forced 3D IGWB in laboratory experiments (Bordes et al. 2012). According to this theoretical model, the mean flow arises from two distinct effects: (i) the presence of 3D beam variations, much as the mean flow induced by a nonlinear modulated wavepacket, where viscous dissipation plays

no role (Tabaei and Akylas 2007); and (ii) viscous attenuation along the beam propagation direction, similar to the acoustic streaming due to dissipating wavetrains (Lighthill 1978).

Here, we use the beam–mean-flow interaction model derived in KA to examine the stability of IGWB to 3D perturbations. This also makes it possible to explore the role of the two mean-flow generation mechanisms identified above in causing instability.

2. 数理モデル

The asymptotic model of KA applies to small-amplitude thin beams with large-scale along-beam and transverse variations. Briefly, assuming that nonlinear, dispersive and viscous damping effects are weak and equally important, the beam–mean-flow interaction equations (in normalized form such that the dependence on the beam inclination to the horizontal is scaled out) are

$$U_T + \overline{V}U_\eta + \mathrm{i}\left(\int^\eta U_X \mathrm{d}\eta' + \int^\eta \int^{\eta'} U_{ZZ}\mathrm{d}\eta''\mathrm{d}\eta' \right) - \beta U_{\eta\eta} = 0, \tag{1}$$

$$\frac{\partial \overline{V}}{\partial T} = \mathrm{i}\frac{\partial}{\partial Z}\mathcal{H}\left[\int_{-\infty}^\infty \left\{ \frac{1}{2}\left(U^*U_\eta\right)_T + \beta U_\eta^* U_{\eta\eta} \right\} \mathrm{d}\eta \right]. \tag{2}$$

Here, $U(X,\eta,Z,T)$ is the complex amplitude of the beam velocity component in the along-beam (X-) direction, $\overline{V}(X,Z,T)$ is the induced mean-flow component in the across-beam (η-) direction, Z is the transverse horizontal coordinate and T is the slow (relative to the beam period) evolution time. Also, $\mathcal{H}$ stands for the Hilbert transform in Z, * denotes complex conjugate and the parameter β controls viscous dissipation. Equations (1), (2) form a closed system for U and $\overline{V}$, to be solved subject to the boundary conditions

$$\int^\eta \int^{\eta'} U \,\mathrm{d}\eta''\mathrm{d}\eta' \to 0 \quad (\eta \to \pm\infty), \tag{3}$$

which ensure that the beam velocity field remains locally confined in the beam vicinity, $\eta = O(1)$. On the other hand, $\overline{V}$, which is uniform in η, must be matched to a far-field ($|\eta| \gg 1$) mean-flow solution, that ultimately decays away from the beam. Detailed derivation of (1)–(3) and this matching procedure are presented in KA.

It should be noted that transverse (Z-) beam variations are key to the nonlinear coupling of U and $\overline{V}$ in (1), (2). Moreover, the two terms on the right-hand side of (2) represent, respectively, the modulation and viscous streaming mechanisms of mean-flow generation, noted

in §1. In the following, we discuss how each of these mechanisms may instigate 3D instability of IGWB.

3. 変調不安定

Throughout this section we focus on the inviscid limit ($\beta = 0$), where from (2)

$$\overline{V} = \frac{\mathrm{i}}{2} \frac{\partial}{\partial Z} \mathcal{H}\left[\int_{-\infty}^{\infty} U^* U_\eta \mathrm{d}\eta\right]. \tag{4}$$

The induced mean flow is thus 'slaved' to the beam amplitude evolution, which is governed by (1) with $\overline{V}$ given by (4). A particular 2D solution of this reduced system is

$$U = U_B = F(\eta) + G(\eta + bX)\mathrm{e}^{-\mathrm{i}bT}, \quad \overline{V} = 0. \tag{5}$$

This represents the superposition of two nearly parallel free uniform beams with profiles F, G and slightly different frequencies, controlled by the choice of the constant b.

We wish to examine the stability of the 2D state (5) to infinitesimal 3D perturbations. Since U_B is independent of Z and periodic in T, by Floquet theory, the perturbed state is taken in the form

$$U = U_B + \sum_{n=-\infty}^{\infty}\left\{u_n(X,\eta)\mathrm{e}^{\mathrm{i}\left(lZ-(\omega+nb)T\right)} + u_n'^*(X,\eta)\mathrm{e}^{-\mathrm{i}\left(lZ-(\omega^*+nb)T\right)}\right\}, \tag{6a}$$

$$\overline{V} = \sum_{n=-\infty}^{\infty}\left\{v_n(X)\mathrm{e}^{\mathrm{i}\left(lZ-(\omega+nb)T\right)} + \text{c.c.}\right\}. \tag{6b}$$

Upon substituting (6) in (1), (4) and linearizing with respect to the perturbation, we obtain an eigenvalue problem (EVP) for u_n, u_n' and v_n ($-\infty < n < \infty$), with $\omega = \omega_r + \mathrm{i}\omega_i$ being the eigenvalue. This EVP can be greatly simplified by introducing the Fourier transform in X and η,

$$u_n(X,\eta) \leftrightarrow \tilde{u}_n(k,l), \quad u_n'(X,\eta) \leftrightarrow \tilde{u}_n'(k,l), \quad v_n(X) \leftrightarrow \tilde{v}_n(k). \tag{7}$$

Then, it is possible to eliminate $\tilde{u}_n$ and $\tilde{u}_n'$ and finally obtain the following EVP for $\tilde{v}_n$ ($-\infty < n < \infty$) alone:

$$I(\omega+nb,k)\tilde{v}_n(k) = \int_{-\infty}^{\infty}\left[J(\omega+nb,k,l)\tilde{v}_{n-1}(k-lb) + K(\omega+nb,k,l)\tilde{v}_{n+1}(k+lb)\right]\mathrm{d}l, \tag{8}$$

where

$$I(\omega,k) = \frac{1}{2\pi^4} - \int_{-\infty}^{\infty} \frac{\left|\widetilde{F}(l')\right|^2 + \left|\widetilde{G}(l')\right|^2}{\left(\omega - \dfrac{k}{l'}\right)^2 - \dfrac{\pi^4}{l'^4}}\,\mathrm{d}l',$$

$$J(\omega,k,l) = \frac{\widetilde{F}^*(l)\widetilde{G}(l)}{\left(\omega - \dfrac{k}{l}\right)^2 - \dfrac{\pi^4}{l^4}}, \quad K(\omega,k,l) = \frac{\widetilde{F}(l)\widetilde{G}^*(l)}{\left(\omega - \dfrac{k}{l}\right)^2 - \dfrac{\pi^4}{l^4}}. \tag{9}$$

It should be noted that the right-hand side of (8) vanishes when the two beams propagate in *opposite* directions because the beam profiles F, G involve only wavenumbers of opposite signs (Tabaei et al. 2005), so $\widetilde{F}^*(l)\widetilde{G}(l) = \widetilde{F}(l)\widetilde{G}^*(l) = 0$. The eigenvalue condition in this instance then reduces to

$$I(\omega,\kappa) = 0, \tag{10}$$

for given $k = \kappa$. Moreover,

$$\widetilde{v}_n(k) = \begin{cases} V_0 \delta(k - \kappa) & (n = 0) \\ 0 & (n \neq 0). \end{cases} \tag{11}$$

Thus, the eigenvalues ω, determined by (10), as well as the eigenmode $\widetilde{v}_n$ in (11) are independent of the parameter b, and hence the difference in inclination to the horizontal of the two beams. Although at first sight this may seem counterintuitive, we recall that the induced mean flow, which is responsible for an instability, extends far from the vicinity of the beams.

When the two beams propagate in the *same* direction, the right-hand side of (8) does not vanish and the solution of the EVP is more complicated. However, in the simplest case of two parallel beams ($b = 0$), the eigenmode $\widetilde{v}_n$ is still given by (11) and the eigenvalue condition takes the form

$$I(\omega,\kappa) = \int_{-\infty}^{\infty} \left[J(\omega,\kappa,l) + K(\omega,\kappa,l)\right]\mathrm{d}l. \tag{12}$$

The EVP solution for $b \neq 0$ will be discussed elsewhere.

First, we report results on the stability of two interacting beams propagating in *opposite* directions, where there is no dependence on b. We specifically consider two identical Gaussian beams:

$$F(\eta) = U_G(\eta), \quad G(\eta) = U_G^*(\eta), \tag{13}$$

where

$$U_G(\eta) = \frac{U_0}{\sqrt{8\pi}} \int_0^\infty il \exp\left(-\frac{l^2}{8} + il\eta\right) dl, \tag{14}$$

with U_0 being a parameter that controls the beam peak amplitude. The eigenvalues $\omega = \omega_r + i\omega_i$ were computed numerically from (10), with $\omega_i > 0$ implying instability. The growth rates ω_i versus κ are plotted in figure 1. Only results of the greatest growth rate ω_i, corresponding to the most unstable mode, for given U_0 and κ are presented.

Next, we show results on the stability of two parallel ($b = 0$) beams propagating in the *same* direction. Specifically, we consider two identical Gaussian beams separated by a distance D:

$$F(\eta) = U_G(\eta - D/2), \quad G(\eta) = U_G(\eta + D/2). \tag{15}$$

The eigenvalues $\omega = \omega_r + i\omega_i$ were computed numerically from (12), and the growth rates ω_i versus κ are plotted in figure 2 for $D = 2$, 4 and 10. As expected, both for beams propagating in the same and opposite directions, the predicted instability becomes stronger as the beam amplitude is increased. Also, for parallel beams propagating in the *same* direction, instability arises for D larger than about 1.5 and the maximum growth rate is reached when $D = 4$. On the other hand, surprisingly enough, neither b nor D affects the stability of two counterpropagating beams.

We also studied the *transient* development of forced beams by solving numerically (1) and (4), with the addition of the following forcing terms on the right-hand side of (1):

$$i\int^\eta \{F(\eta') + G(\eta')\} d\eta' \, \delta(X) \quad \text{for 2D calculation,} \tag{16}$$

$$i\int^\eta \{F(\eta') + G(\eta')\} d\eta' \, \delta(X)(1 + 0.03\cos \pi Z) \quad \text{for 3D calculation.} \tag{17}$$

The results of our simulations are summarized in figure 3. From the results in figures 1 and 2, two parallel beams of amplitude $U_0 = 2$ separated by a distance $D = 4$ are expected to be unstable to 3D perturbations, and this is clearly confirmed in figure 3(b, c). It should be noted that the instability is brought about solely by the beam interaction, as a single forced beam, in the presence of the same 3D perturbation, propagates stably (figure 3a). Moreover, the result of this 3D instability is quite dramatic as it destroys the identity of the interacting beams.
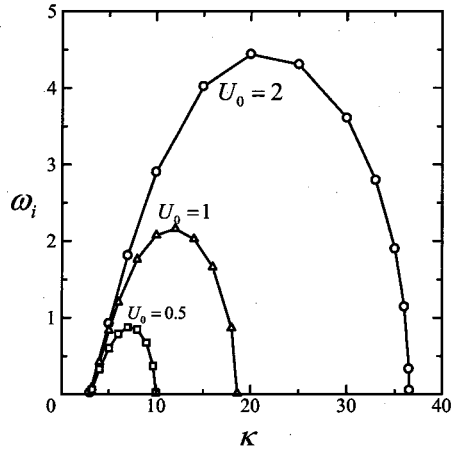
Figure 1: Computed growth rates ω_i versus κ for two beams propagating in *opposite* directions. The beam peak amplitudes are chosen to be $U_0 = 0.5$, 1, and 2. Here, the stability results are independent of the inclination parameter b, as well as the separation distance D if the two beams are parallel ($b = 0$).
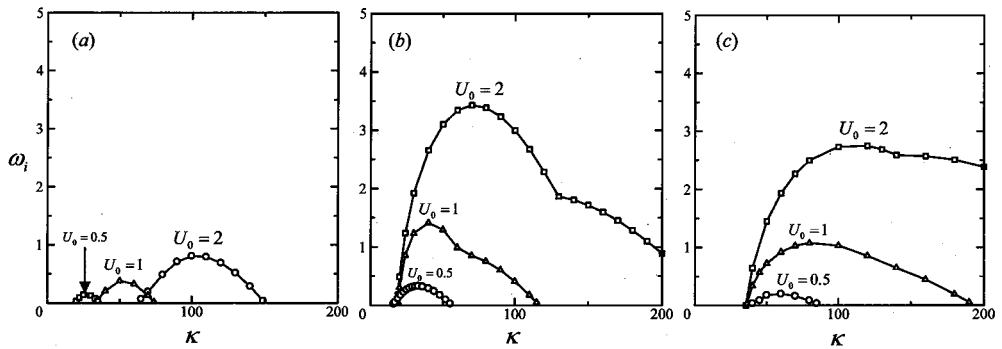
Figure 2: Computed growth rates ω_i versus κ for two parallel ($b = 0$) beams separated by a distance D and propagating in the *same* direction: (a) $D = 2$, (b) $D = 4$, (c) $D = 10$. The beam peak amplitudes are chosen to be $U_0 = 0.5$, 1 and 2.
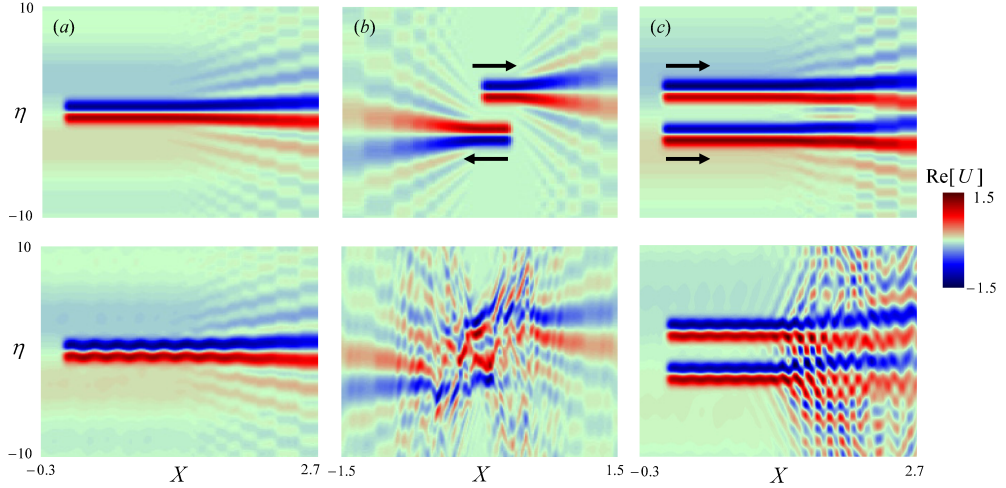
Figure 3: Vertical flow slice at $Z = 0$ of beam amplitude U (only the real part is shown) for (a) single propagating beam (at time $T = 7$), (b) two parallel beams ($D = 4$) propagating in *opposite* directions (at time $T = 2$), (c) two parallel beams ($D = 4$) propagating in the *same* direction (at time $T = 7$). In all cases the beam peak amplitude $U_0 = 2$. The top and bottom figures are, respectively, 2D calculation with the forcing term (16) and 3D calculation with the forcing term (17). Viscous effects are ignored ($\beta = 0$).
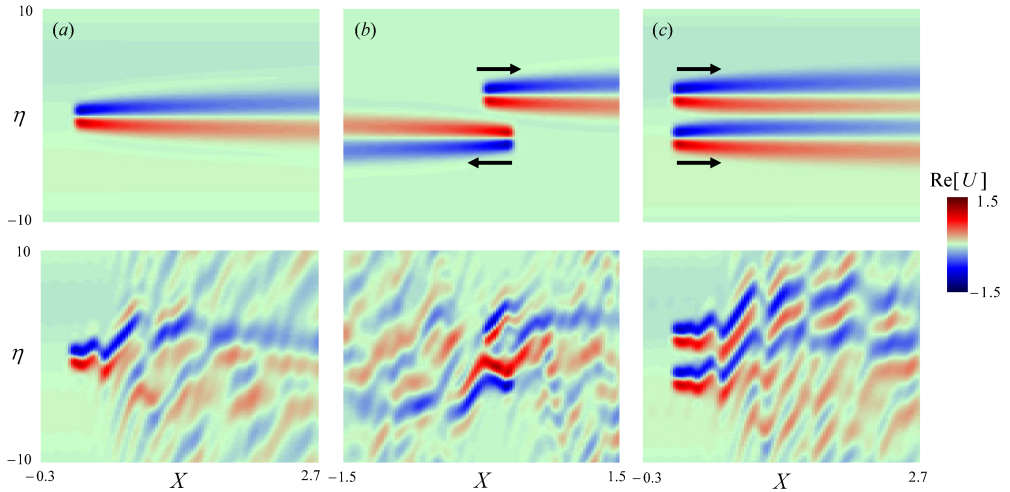

Figure 4: Vertical flow slice at $Z = 0$ of beam amplitude U (only the real part is shown) for viscous parameter $\beta = 0.1$ and (a) single propagating beam (at time $T = 7$), (b) two parallel beams ($D = 4$) propagating in *opposite* directions (at time $T = 4$), (c) two parallel beams ($D = 4$) propagating in the *same* direction (at time $T = 7$). In all cases the beam peak amplitude $U_0 = 2$. The top and bottom figures are, respectively, 2D calculation with the forcing term (16) and 3D calculation with the forcing term (17).

4. 粘性の影響

The effects of viscosity on the transient behavior of forced beams were explored by solving numerically (1) (with the addition of the forcing terms (16) or (17)) and (2), for three different values of the parameter $\beta = 0.01, 0.1$ and 1. It turns out that the effects of viscous streaming — represented by the second term on the right-hand side of (2) — are most dramatic for the moderately viscous case $\beta = 0.1$. The corresponding simulation results are shown in figure 4. It is seen that viscous streaming leads to significant distortion even for a single propagating beam which is stable in the inviscid limit (figure 3a).

5. 結言

The preceding analysis has shown that, depending on the beam profile and amplitude, a single isolated uniform IGWB as well as two interacting uniform IGWB which propagate in the same or opposite directions, can be subject to 3D modulational instability brought about by a purely inviscid nonlinear mechanism. Moreover, for moderate viscous dissipation, the mean flow induced by a mechanism analogous to acoustic streaming can cause significant distortion, leading to breakdown, of forced IGWB with small lateral amplitude variations. These findings suggest that modulational and streaming instabilities are central to 3D IGWB dynamics, in constrast to the widely-studied PSI of sinusoidal wavetrains (Staquet and Sommeria 2002), which is most relevant to beams with nearly monochromatic profile only (Karimi and Akylas 2014).

参考文献

Bordes, G., Venaille, A., Joubaud, S. Odier, P. and Dauxois, T. (2012). Experimental observation of a strong mean flow induced by internal gravity waves. *Phys. Fluids*, 24:086602.

Karimi, H. H. and Akylas, T. R. (2014). Parametric subharmonic instability of internal waves: locally confined beams versus monochromatic wavetrains. *J. Fluid Mech.*, 757:381–402.

Kataoka, T. and Akylas, T. R. (2015). On three-dimensional internal gravity wave beams and induced large-scale mean flows. *J. Fluid Mech.*, 769:621–634.

Lighthill, M. J. (1978). Acoustic streaming. *J. Sound Vib.*, 61:391-418.

Staquet, C. and Sommeria, J. (2002). Internal gravity waves: from instabilities to turbulence. *Ann. Rev. Fluid Mech.*, 34:559–593.

Tabaei, A. and Akylas, T. R. (2003). Nonlinear internal gravity wave beams. *J. Fluid Mech.*, 482:141–161.

Tabaei, A. and Akylas, T. R. (2007). Resonant long–short wave interactions in an unbounded rotating stratified fluid. *Stud. Appl. Math.*, 119:271–296.

Tabaei, A., Akylas, T. R. and Lamb, K. G. (2005). Nonlinear effects in reflecting and colliding internal wave beams. *J. Fluid Mech.*, 526:217–243.